Available online at www.sciencedirect.com
ScienceDirect
Polymer 48 (2007) 6782–6790
polymer
www.elsevier.com/locate/polymer

Synthesis and formation mechanism study of rectangular-sectioned polypyrrole micro/nanotubules

Wei Yan*, Jie Han

Department of Environmental Science and Engineering, Xi'an Jiaotong University, Xi'an 710049, People's Republic of China

Received 13 May 2007; received in revised form 18 September 2007; accepted 20 September 2007
Available online 23 September 2007

Abstract

Aligned polypyrrole (PPy) micro/nanotubules were synthesized via a self-assembly method using $FeCl_3$ as oxidant and Acid Red 1 (C.I. 18050, 5-(acetylamino)-4-hydroxy-3-(phenylazo)-2,7-naphthalenedisulfonic acid) as dopant. PPy has a typical length of 530 μm and a unique rectangular-sectioned morphology. Its general morphology could be manipulated by varying synthetic conditions including polymerization time, monomer concentration, oxidant species, and stirring. The synthesized PPy and reaction intermediates were characterized by scanning electron microscopy (SEM), transmission electron microscopy (TEM), X-ray powder diffraction (XRD), and solubility tests in methanol and water. Our observation and results suggest a plausible formation mechanism of rectangular-sectioned PPy micro/nanotubules. AR1–Fe(II) complex formed from the complexation of Acid Red 1 and Fe^{2+}(reduced from Fe^{3+}), which precipitated in the aqueous solution, might have functioned as 'template' during the polymerization of pyrrole monomers. The conductivity of PPy with different morphologies was also measured and compared.

Keywords: Polypyrrole; Rectangular; Micro/nanotubules

1. Introduction

Intrinsically conducting polymers have gained wide attentions for their unique electroactive properties and potential applications in molecular electronics [1,2], electrical displays [3,4], chemical and biomedical sensors [5–7], and drug delivery [8]. Particularly, conducting polymer micro/nanotubular structures are of great interests for their metal-like conductivity. They are excellent templates or 'micro/nanoreactors' to manufacture molecular wires or rings which are elements of molecular devices [9]. On the other hand, among the conductive polymers, polypyrrole (PPy) is one of the most extensively studied conducting polymers for its high conductivity and long-term environmental stability [10–12].

Previous studies have used template-synthesis method to prepare PPy micro/nanostructures [13–16]. A typical template-synthesis process uses a microporous or nanoporous membrane as a template to control the PPy structure during the polymerization, which also needs to be removed after the synthesis. Wan's group [9,17–20] developed a self-assembly method and prepared PPy and polyaniline (PANI) micro/nanotubules. Because of not using external template, the self-assembly method has been considered a convenient way to prepare conducting polymer micro/nanotubules [21–23].

Despite of its simplicity, self-assembly method has not been widely applied because the morphology of PPy tubules fabricated by self-assembly method is generally unsatisfactory comparing to those obtained by template-synthesis. The self-assembly method has the advantage of simplicity and potentially lower cost, but it also has the difficulty in manipulating the morphology of product due to the absence of template during the synthesis. Previously synthesized PPy and PANI tubules using self-assembly method [9,17–23] were exclusively cylindrical, with a typical length less than 100 μm [19,20,22]. Synthesis of PPy micro/nanotubules with rectangular sections or longer length has not been achieved so far via the self-assembly method. However, long conducting polymer

* Corresponding author. Tel.: +86 29 82664731.
E-mail address: yanwei@mail.xjtu.edu.cn (W. Yan).

0032-3861/$ - see front matter © 2007 Elsevier Ltd. All rights reserved.
doi:10.1016/j.polymer.2007.09.026

tubules are preferred as long tubules can be easily tailored for various applications but insufficient length will limit their applications. In addition, PPy micro/nanotubules with rectangular sections may be highly desirable for some uses because the remarkable rectangular-sectioned micro/nanotubules may exhibit exceptional optical and mechanical properties that are not achievable in circular PPy micro/nanotubules [24].

To our best knowledge, the synthesis of rectangular PPy tubules has not been reported yet except in our previous study [25]. In this paper, we synthesized PPy with different morphologies, i.e. granular, cylindrical, and rectangular-sectioned micro/nanotubules, by controlling synthetic conditions in a self-assembly process. The formation mechanism of rectangular-sectioned PPy micro/nanotubules was studied by characterizing resultant PPy and reaction intermediates sampled at various conditions. The conductivity of PPy rectangular-sectioned micro/nanotubules, cylindrical micro/nanotubules, and granule was also measured and discussed.

2. Experimental

2.1. Materials

Pyrrole (98%, Sigma–Aldrich) monomers were distilled at reduced pressure. The treated pyrrole was refrigerated and stored in the dark under the protection of nitrogen. Acid Red 1 (5-(acetylamino)-4-hydroxy-3-(phenylazo)-2,7-naphthalenedisulfonic acid) was purchased from Aldrich and was used as dopant in the synthesis. The molecular structure of Acid Red 1 is shown in Fig. 1. The sulfonic groups provide the hydrophilicity of Acid Red 1, and the hydroxyl and azo groups adjacent to the naphthol ring are strong ligands which could form complexes with transitional metal ions [26]. The as-received Acid Red 1 was purified by repeated crystallization in methanol before use. Ferric chloride hexahydrate ($FeCl_3 \cdot 6H_2O$, ≥98%, Beijing Chemicals), ferrous chloride tetrahydrate ($FeCl_2 \cdot 4H_2O$, 99%, Beijing Chemicals), methanol (anhydrous, 99.8%, Aldrich), and ammonium persulfate (APS, ≥98%, Fluka) were used as-received.

2.2. Preparation

The synthesis process of the rectangular-sectioned PPy micro/nanotubules was as follows: 1 mol L^{-1} $FeCl_3$ aqueous solution was prepared by dissolving ferric chloride hexahydrate ($FeCl_3 \cdot 6H_2O$) in deionized water. The prepared $FeCl_3$ solution was used as the oxidant. Pyrrole monomer of 20 mmol (1.4 mL) and 4 mmol Acid Red 1 were dissolved in 30 mL deionized water with vigorous magnetic stirring for 30 min. A total amount of 33.4 mL of the prepared $FeCl_3$ solution was added dropwise into the solution for 2 h without stirring at 278 K. The resultant mixture was allowed to stand for 24 h. The precipitated PPy solids were filtered and washed with a large volume of deionized water until the filtrate became colorless. The PPy solids were further purified by a soxhlet extraction using methanol as the solvent until the extraction solution became colorless. The obtained PPy solids were dried in vacuum oven for 12 h at 298 K.

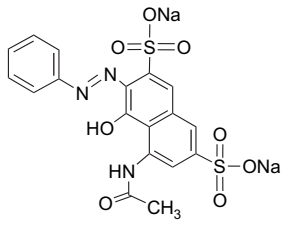

Fig. 1. The molecular structure of the dopant Acid Red 1.

Experimental conditions were varied to investigate their influences on the morphology of resultant PPy. The effect of polymerization time was investigated by allowing the reaction to stand for 2, 4, and 24 h respectively, and examining the morphology of resultant PPy. Other conditions were unchanged. The effect of pyrrole concentration was studied at two initial monomer concentrations (0.31 and 0.15 mol L^{-1}) with other conditions unchanged. The influence of oxidant was investigated by replacing the 33.4 mL of 1 mol L^{-1} $FeCl_3$ solution with 33.4 mL of 0.5 mol L^{-1} ammonium persulfate (APS) solution with other conditions unchanged.

To study the formation mechanism of rectangular-sectioned PPy micro/nanotubules, two Acid Red 1 solutions were prepared separately by dissolving 4 mmol Acid Red 1 into 30 mL deionized water; 33.4 mmol $FeCl_2 \cdot 4H_2O$ and 33.4 mmol $FeCl_3 \cdot 6H_2O$ were added into the Acid Red 1 solutions for 2 h with gentle stirring. The precipitated solids in two solutions, designated as AR1–Fe(II) and AR1–Fe(III), were filtered and washed with deionized water. The solubility of AR1–Fe(II) was tested in deionized water and methanol, respectively.

2.3. Characterization

Morphologies of PPy obtained at different experimental conditions were examined by transmission electron microscope (TEM, Hitachi JEM-200CX), scanning electron microscope (SEM, Hitachi-530), and field emission scanning electron microscope (FESEM, JEOL JSM-6700F). AR1–Fe(II) and AR1–Fe(III) solids were characterized by SEM. The synthesized rectangular-sectioned PPy micro/nanotubules (unwashed and methanol-washed), AR1–Fe(II), and AR1–Fe(III) solids were examined by powder X-ray diffraction (XRD) on a Rigaku D/Max-2400X X-ray diffractometer with Cu Kα radiation. The conductivity of PPy was measured by the four-probe method using a Keithley 196 SYSTEM DMM digital multimeter, and an ADVANTEST R6142 programmable DC voltage/current generator as the current source. All conductivity measurements were conducted at room temperature.

3. Results and discussion

3.1. Morphology

Fig. 2 shows the morphology of synthesized PPy micro/nanotubules. In Fig. 2(a) and (b), most PPy tubules have

rectangular cross-sections except a few cylindrical tubules. The TEM image of PPy in Fig. 2(c) shows the hollow inner structure of these PPy tubules. Dimensions of the rectangular-sectioned PPy micro/nanotubules were estimated as: 530 μm in average length, 150–2000 nm in side length, and 50 nm in wall thickness [25]. The unique rectangular-sectioned morphology is different from the cylindrical PPy tubules reported in previous studies. Additionally, the rectangular-sectioned PPy tubules are exceptionally longer than PPy tubules obtained with self-assembly methods in pervious studies which ranged from 2 to 100 μm [19,20,22] and also longer than many PPy tubules synthesized by template method [27–29].

3.2. Factors influencing morphology

3.2.1. Reaction time

Fig. 3 shows the SEM images of PPy obtained after different polymerization times. As seen from Fig. 3(a), PPy shows a belt-like morphology with a few cylindrical tubules and some granules which failed to form the 'belt' at the initial stage ($t = 2$ h). A high-resolution SEM image (Fig. 3(b)) taken at the fracture and the end of these 'belts' confirms that these belts are actually shriveled tubules. Fig. 3(c) shows the rectangular-sectioned PPy tubules obtained after 4 h polymerization. However, it should be noted that these rectangular tubules have thin walls and one of them is metamorphosed at the end. Belt-like PPy can also be found in Fig. 3(c). Based on these observations, it is implied that: (1) during the polymerization, PPy grew to form the micro/nanotubules not only through elongation [30] but also through accretion [31]; (2) the metamorphosis of rectangular-sectioned PPy micro/nanotubules was attributed to the operation of drying in the vacuum oven. At the initial stage ($t = 2$ h), the PPy tubules had thin walls which were easily shriveled into 'belts' during the vacuum drying. During the polymerization, the walls of these tubules became thicker and more compact. It is clear that the obtained PPy tubules have a rectangular-sectioned morphology with compact walls after 24 h polymerization, as shown in Fig. 3(d). These tubules could not be easily metamorphosed into 'belts' during the vacuum drying process.

3.2.2. Concentration of pyrrole

The initial concentration of pyrrole monomer was considered as a potential influencing factor on the morphology of synthesized PPy micro/nanotubules. In this study, two concentration levels were chosen (0.31 and 0.15 mol L^{-1}) to investigate the effect of pyrrole concentration. Fig. 4 shows the morphology of the PPy micro/nanotubules synthesized with different concentrations of pyrrole monomers. It is found that the PPy tubules synthesized with 0.31 mol L^{-1} pyrrole have compact walls (Fig. 4(a)), while there are cavities distributing uniformly on the walls of PPy tubules when the concentration

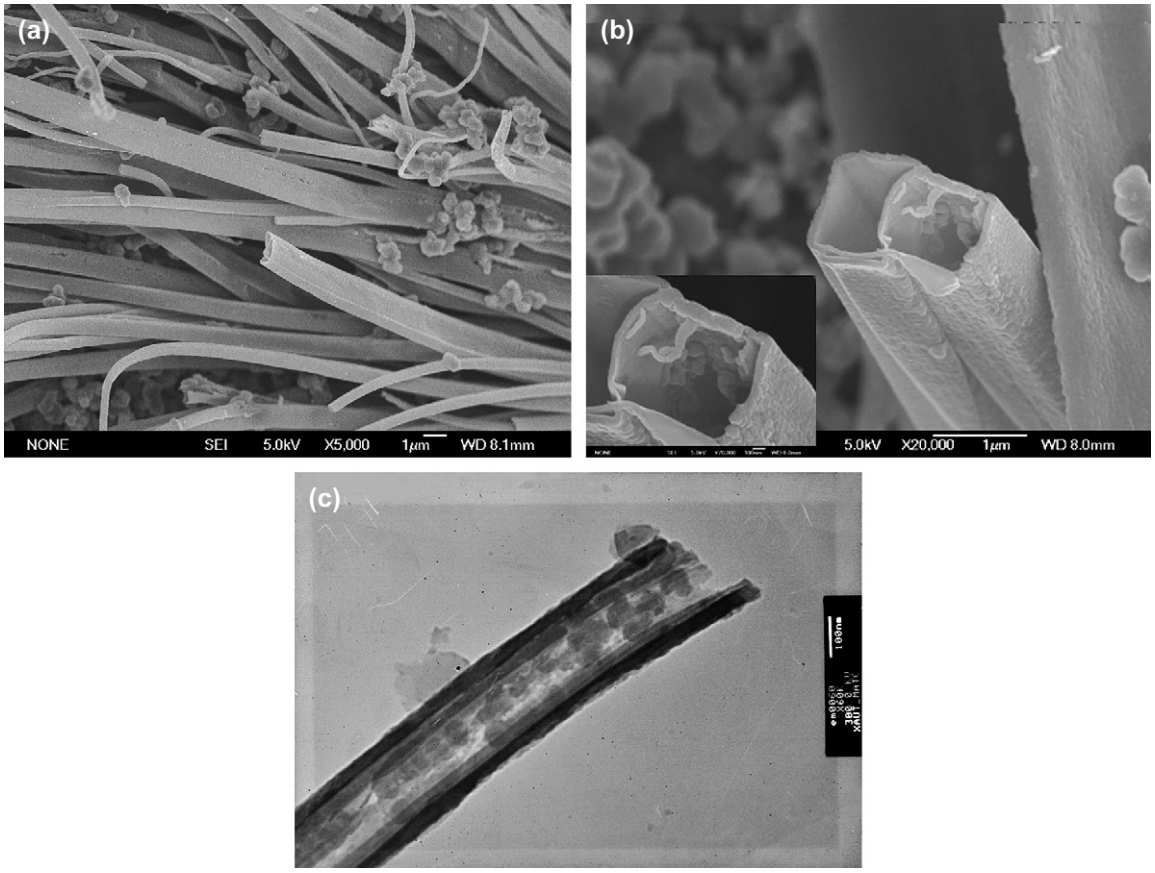

Fig. 2. (a) and (b) SEM images and (c) TEM image of the synthesized rectangular-sectioned PPy micro/nanotubules (pyrrole: 0.31 mol L^{-1}, Acid Red 1: 0.062 mol L^{-1}, $FeCl_3$: 0.52 mol L^{-1}, 278 K, no stirring).

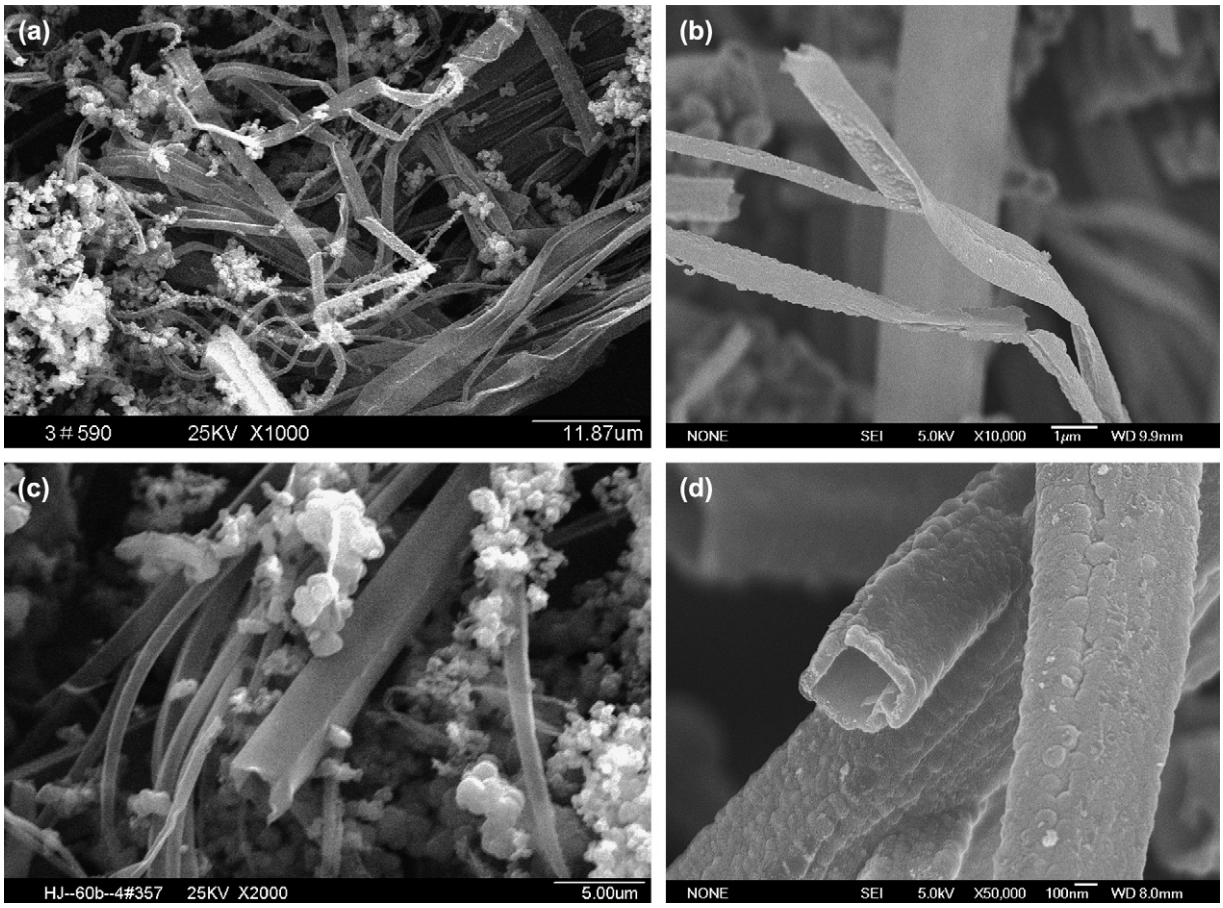

Fig. 3. Morphology of the PPy micro/nanotubules synthesized in (a) and (b) 2 h; (c) 4 h; and (d) 24 h (pyrrole: 0.31 mol L^{-1}, Acid Red 1: 0.062 mol L^{-1}, $FeCl_3$: 0.52 mol L^{-1}, 278 K, no stirring).

of pyrrole monomer was reduced to 0.15 mol L^{-1} (Fig. 4(b)). It is thus concluded that the concentration of pyrrole monomers should be sufficiently high to ensure that compact walls could be formed in PPy micro/nanotubules.

3.2.3. Oxidant

Ammonium persulfate (APS, >98.0%, Fluka) was used as the oxidant to replace $FeCl_3$ to study the influence of oxidant species in the synthesis. Other experimental conditions were unchanged, i.e. pyrrole: 0.31 mol L^{-1}, Acid Red 1: 0.062 mol L^{-1}, APS: 0.26 mol L^{-1}, 278 K, no stirring. As shown in Fig. 5, granular PPy was obtained when APS was used as the oxidant. This result demonstrates that the presence of $FeCl_3$ in the reaction was indispensable for the formation of rectangular-sectioned PPy micro/nanotubules. It is also implied that the unique rectangular-sectioned morphology of resultant PPy tubules was associated to the interaction between the oxidant and the dopant (Acid Red 1). This assumption was further discussed in Section 3.3 with characterization results.

3.2.4. Stirring

The rectangular-sectioned PPy micro/nanotubules were obtained under no stirring condition. Interestingly, when the reaction solution was stirred ($r \geq 200$ rpm), PPy micro/nanotubules with hollow cylindrical morphology were obtained. Fig. 6 shows that these PPy tubules have morphology similar to the tubular PPy synthesized by Wan and Liu [9] using beta-naphthalenesulfonic acid (β-NSA) as dopant in a self-assembly process. In Wan's study, β-NSA was considered as an anionic surfactant which formed micelles in aqueous solution under vigorous stirring. The β-NSA micelles acted as templates where pyrrole monomers polymerized and cylindrical PPy micro/nanotubules formed. Likewise, Acid Red 1 has both hydrophilic and hydrophobic groups which tend to form micelles in aqueous reaction solution under a vigorous-stirring condition and these micelles could act as templates during the formation of cylindrical PPy micro/nanotubules. The similar reaction mechanism was reported in Jang's literature, which used sodium bis(2-ethylhexyl) sulfosuccinate (AOT) as surfactant to synthesis poly(3,4-ethylenedioxythiophene) (PEDOT) nanorods and nanotubes [32]. However, it should be noted that the rectangular-sectioned PPy micro/nanotubules were obtained under no stirring, which means that the uniform-sized micelles were difficult to form in the solution. Also, as micelles are generally spherical or cylindrical [33,34], they were unlikely to be the templates for the rectangular-sectioned PPy tubules. It is thus implied that the micelles of dopants (Acid Red 1) and monomers (pyrrole) were not the templates for the rectangular-sectioned PPy tubules and their formation might have followed a different mechanism from literature [9].

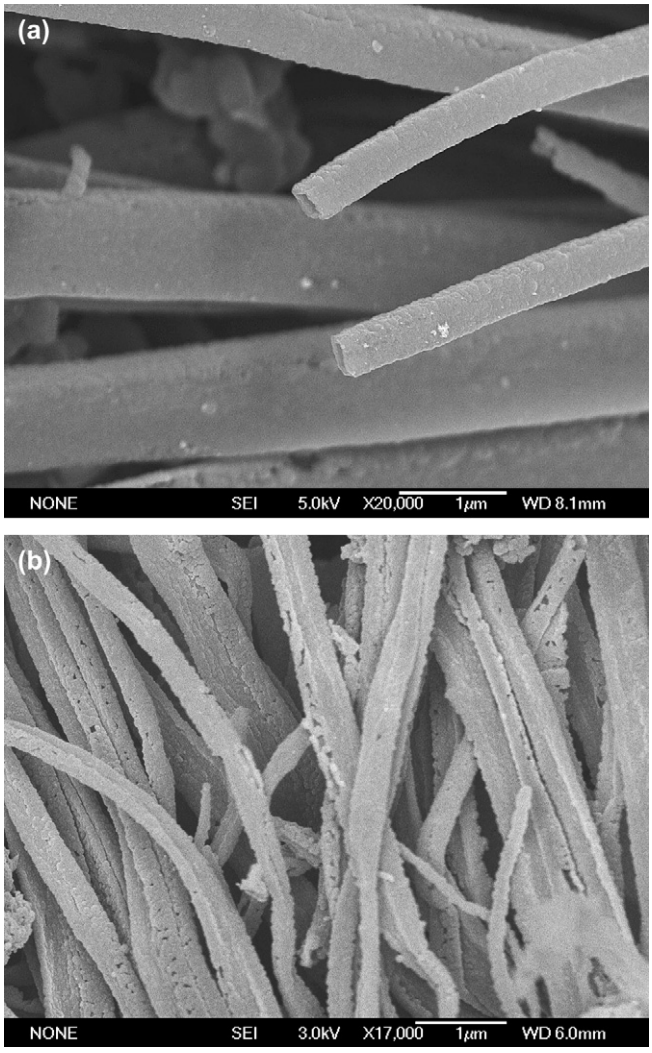

Fig. 4. Morphology of the rectangular-sectioned PPy micro/nanotubules synthesized with pyrrole concentration of (a) 0.31 mol L^{-1} or (b) 0.15 mol L^{-1} (Acid Red 1: 0.062 mol L^{-1}, $FeCl_3$: 0.52 mol L^{-1}, 278 K, no stirring).

3.3. Formation mechanism

It is implied that the morphology of the rectangular-sectioned PPy tubules was determined by certain crystals in tetragonal shapes. To verify the assumption, we examined the morphology of unwashed samples of rectangular-sectioned PPy tubules. Fig. 7(a) shows the SEM image of the cross-section of synthesized PPy micro/nanotubules before washing with methanol. It is shown that the inner space of the PPy tubules is filled with rectangular-sectioned substances. These substances are not firmly attached to the inner walls of PPy tubules; instead, it appears that they grew separately inside the PPy tubules. The TEM image in Fig. 7(b) shows a similar result that there are solids filled in the inner space of the unwashed PPy tubules. But these PPy tubules appear to be hollow after washing with methanol (Fig. 2(b)). From these results we can conclude that the filling substances can be easily dissolved in methanol but had a low solubility in the aqueous reaction solution.

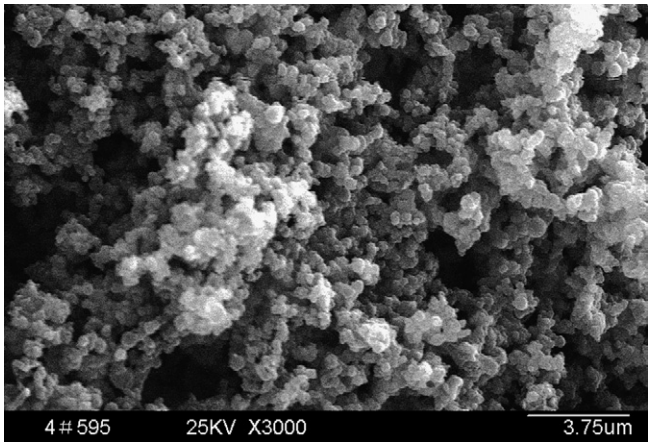

Fig. 5. Granular PPy synthesized with APS as the oxidant (pyrrole: 0.31 mol L^{-1}, Acid Red 1: 0.062 mol L^{-1}, APS: 0.26 mol L^{-1}, 278 K, no stirring).

The reaction process is investigated to identify the filling substances. Firstly, pyrrole monomers were oxidized by $FeCl_3$ in the solution and $FeCl_3$ was reduced into $FeCl_2$. Thus, the filling substances may be the residual Acid Red 1, $FeCl_3$, $FeCl_2$, or the product from their reactions. To study the possible reaction between Acid Red 1 and Fe salts, we prepared the Acid Red 1–$FeCl_3$ solution and the Acid Red 1–$FeCl_2$ solution separately and studied their reaction products. It was observed that there was solid precipitation after 10 h in the $FeCl_3$–Acid Red 1 solution, while the solid precipitation took place after less than 10 min in the $FeCl_2$–Acid Red 1 solution. As shown in Fig. 3(c), rectangular-sectioned PPy tubules with thin walls were formed after 4 h. Since the AR1–Fe(III) solids were produced after 10 h, they could not be the filling substances inside the PPy micro/nanotubules. On the other hand, the AR1–Fe(II) solids which formed quickly in the solution could act as the template during the polymerization of pyrrole monomers.

To identify the filling substance, unwashed and methanol-washed rectangular-sectioned PPy tubules, the AR1–Fe(II)

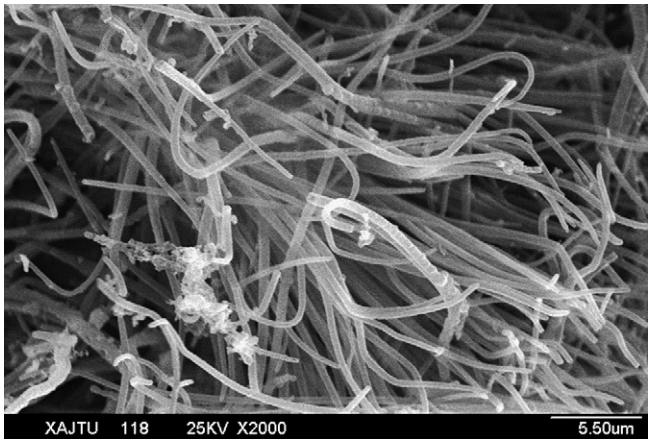

Fig. 6. SEM image of cylindrical PPy micro/nanotubules (pyrrole: 0.31 mol L^{-1}, Acid Red 1: 0.062 mol L^{-1}, $FeCl_3$: 0.52 mol L^{-1}, 278 K, stirring rate $\geq$ 200 rpm).

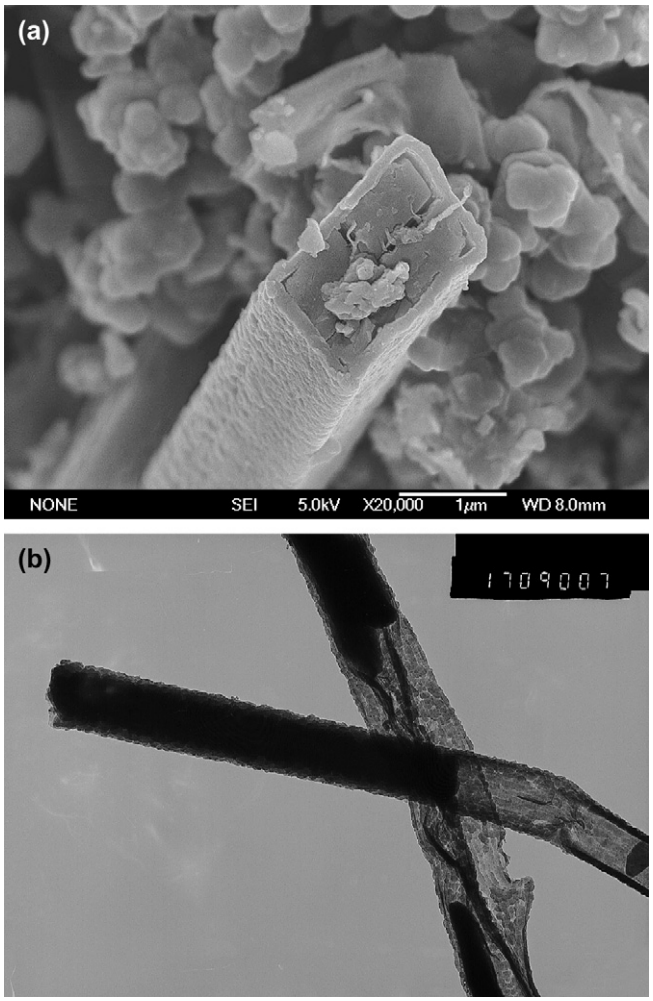

Fig. 7. (a) SEM image and (b) TEM image of the synthesized rectangular-sectioned PPy micro/nanotubules before washing with methanol (pyrrole: 0.31 mol L^{-1}, Acid Red 1: 0.062 mol L^{-1}, $FeCl_3$: 0.52 mol L^{-1}, 278 K, no stirring).

and AR1–Fe(III) solids, pure $FeCl_3$ and $FeCl_2$ solids were analyzed by XRD and the patterns are shown in Fig. 8. Fig. 8(a) and (b) shows the XRD patterns of pure $FeCl_3$ and $FeCl_2$, respectively. Fig. 8(d) and (c) shows the XRD patterns of the unwashed and methanol-washed rectangular-sectioned PPy tubules, respectively. The broad peak in pattern (c) indicates that the PPy tubules are amorphous. By comparing (a)–(d), it can be concluded that there was no pure $FeCl_3$ or $FeCl_2$ existing in the resultant PPy tubules. Fig. 8(e) and (f) shows the XRD patterns of AR1–Fe(II) and AR1–Fe(III) solids, respectively. A direct comparison between (e), (f), and (c) indicates that the characteristic peaks of AR1–Fe(II) complex (pattern (e)) match well with those peaks in the XRD pattern of unwashed PPy tubules (pattern (c)), which confirms that the filling substances in rectangular-sectioned PPy tubules were the AR1–Fe(II) solids, which may be formed by the complexation of Fe^{2+} and Acid Red 1 [35].

It has been well established that the azo functionality coupled with an *ortho*-hydroxyl substituted aromatic group can form extractable complexes with transition metal [35–37].

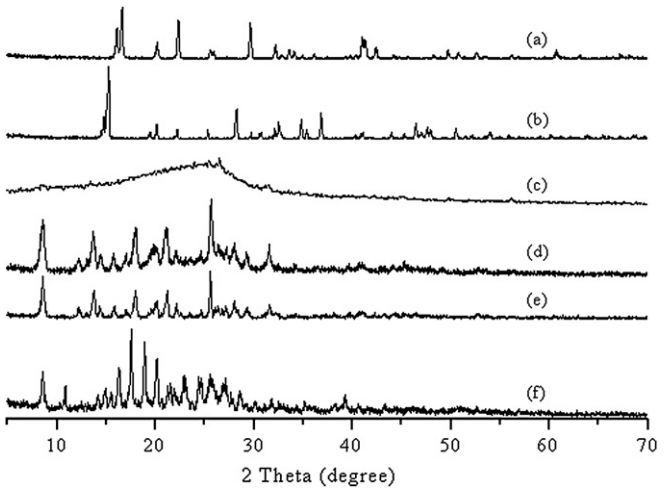

Fig. 8. XRD patterns of (a) $FeCl_2$; (b) $FeCl_3$; (c) rectangular-sectioned PPy micro/nanotubules, methanol-washed; (d) rectangular-sectioned PPy micro/nanotubules, unwashed; (e) AR1–Fe(II); (f) AR1–Fe(III).

In Lu's study the complex formed by the dopant (methyl orange) and the oxide (Fe^{3+}) prior to the polymerization of pyrrole monomers acted as template in forming PPy nanotubules [37b]. In this reaction, Acid Red 1 acted as a ligand and forms metallic complexes through the *ortho*-hydroxyl groups with metal ions in a 2:1 ratio. The structure of the formed metal complexes is illustrated in Fig. 9. In the complex, the phenolic atom, the azo nitrogen atom adjacent to the naphthol ring, and the nitrogen adjacent to the naphthol ring are coordinated to the metal ion. Fig. 10 shows the morphology of AR1–Fe(II) and AR1–Fe(III) complexes. The AR1–Fe(III) complex (Fig. 10(a)) is granular crystal. The AR1–Fe(II) complex (Fig. 10(b)) is tetragonal crystal with dimensions matching well with the rectangular-sectioned PPy tubules. The matching morphology and dimensions of AR1–Fe(II) confirm that the AR1–Fe(II) acted as a 'template' during the polymerization of pyrrole monomers and defined the rectangular-sectioned morphology of resultant PPy tubules.

The solubility of AR1–Fe(II) was tested in water and methanol at 273 K, respectively. Precisely weighed 1.0 g AR1–Fe(II) solids was added to 100 mL deionized water or 100 mL methanol under magnetic stirring. The solubility of AR1–Fe(II) was measured as 30 mg/100 mL water at 273 K. It was observed that the solids dissolved easily in

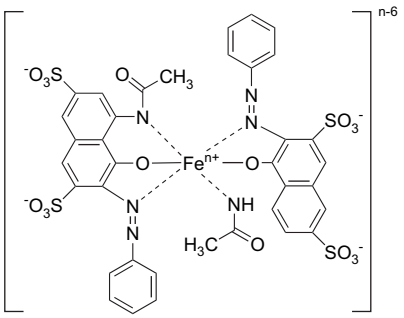

Fig. 9. Structure of the AR1–metal chelates (*n*: valence of the metal cations).

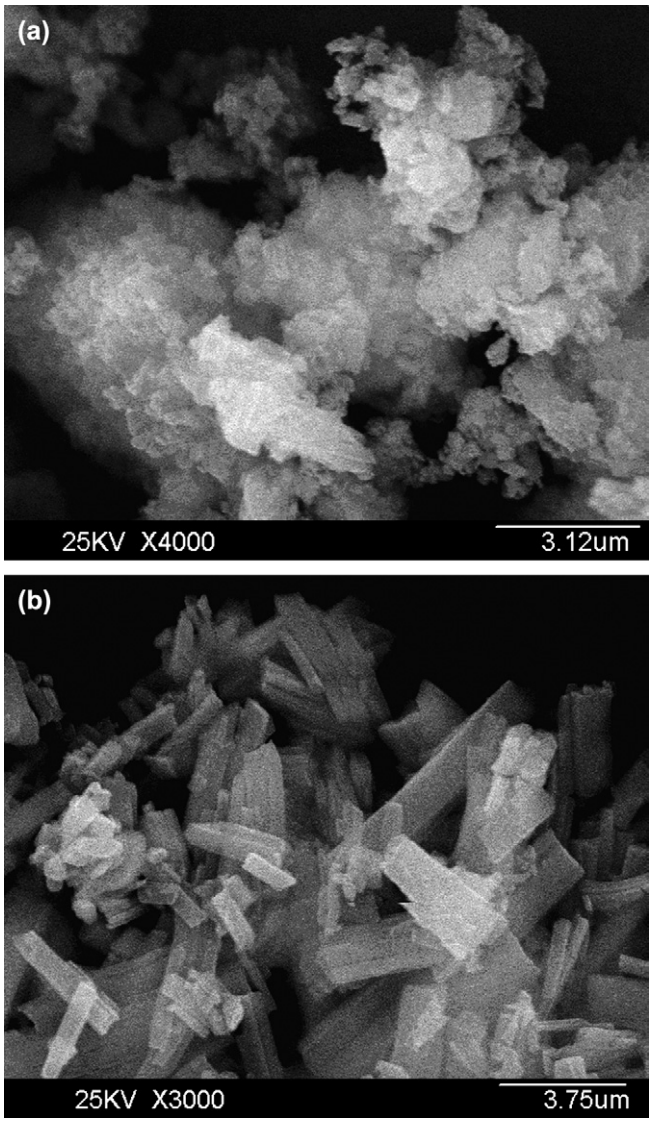

Fig. 10. SEM image of (a) AR1–Fe(III) and (b) AR1–Fe(II).

methanol (solubility > 1 g/100 mL methanol), which agrees with the typically good solubility of similar complexes in methanol [35–37]. The low solubility in water and high solubility in methanol of AR1–Fe(II) are consistent with the observations that the filling substances inside the rectangular-sectioned PPy tubules were insoluble in aqueous solution but were easily removed by washing with methanol. The solubility test results further confirm that the AR1–Fe(II) complex solids were the filling substances inside the rectangular-sectioned PPy micro/nanotubules.

Based on the above discussions, we propose the formation mechanism as follows. The rectangular-sectioned PPy micro/nanotubules were formed by polymerization and continuous growth of pyrrole on the crystals of the AR1–Fe(II) complex. A schematic illustration of the process is presented in Fig. 11. Firstly, pyrrole monomers and Acid Red 1 solution had been adequately stirred, so that the pyrrole monomers were diffused well throughout the mixed solution and Acid Red 1 formed micelles under initial stirring due to its surface activity. When $FeCl_3$ was added dropwise into the solution, the polymerization of pyrrole took place on the interface of Acid Red 1 micelles. Few cylindrical PPy micro/nanotubules formed with the direction of these micelles for the polymerization rate of pyrrole was very fast and AR1–Fe(II) might have not formed at this time. Figs. 2(a) and 3(a) show the existence of these few cylindrical tubules. At the same time, Fe^{3+} ions were reduced into Fe^{2+} ions which quickly reacted with Acid Red 1 by complexation. With Fe^{3+} added continuously more and more AR1–Fe(II) formed. AR1–Fe(II) complex solids were gradually formed as tetragonal crystals in the micelles of Acid Red 1. The tetragonal AR1–Fe(II) crystals, instead of the Acid Red 1 micelles, acted as the templates. Meanwhile, pyrrole monomers continued to polymerize and aggregated on the surface of micelles. PPy gradually deposited on them and the rectangular-sectioned PPy micro/nanotubules were formed by elongation and accretion. Since there was no stirring in the solution, micelles may conglutinate together, which also resulted in some mutual-walled tubules (Fig. 2(b)). When the solution was vigorously stirred, the AR1–Fe(II) crystals might not stay stably inside the Acid Red 1 micelles, which, in turn, destabilized AR1–Fe(II) inside the polymerized pyrrole. As a result, the pyrrole monomers polymerized on the Acid Red 1 micelles. Without the AR1–Fe(II) crystals inside, the Acid Red 1 micelles worked as 'templates' and cylindrical PPy tubules were thus formed.

3.4. Conductivity

The conductivity of rectangular-sectioned PPy tubules was measured to be 28.6 S/cm. The cylindrical PPy tubules show a lower conductivity (21.3 S/cm) and the granular PPy showed a significantly lower conductivity (2.0 S/cm). A comparison with PPy micro/nanotubules reported in literature shows that the rectangular-sectioned PPy tubules have a generally high conductivity among PPy tubules obtained by template-free method, which normally had a conductivity ranged from 10^{-2} to 40 S/cm [9,17–23]. The conductivity of conducting polymer nanostructures is dependent on size variation and alignment [22,38,39]. The relatively high conductivity of rectangular-sectioned PPy tubules can be attributed to the good alignment of tubules, as shown in Fig. 2. The alignment of PPy tubules can greatly affect the conductivity because electron transfer efficiency is dependent on the alignment of conducting polymer tubules [39]. For the size effect, Jang and Yoon [22] reported a slight increment in conductivity (20–30 S/cm) with decreasing diameter of the PPy nanotubules (170–90 nm). Kros et al. [39] also found that larger-diameter nanotubules displayed conductivity comparable to that of bulk PPy, whereas small diameter tubules possessed a conductivity one order of magnitude higher. In our study, the sizes of these rectangular-sectioned PPy tubules ranged from 150 nm to 2 μm. Thus, it is expected that the conductivity of the rectangular-sectioned PPy tubules can be further improved by reducing the sizes and narrowing the size distribution, which is under further study.

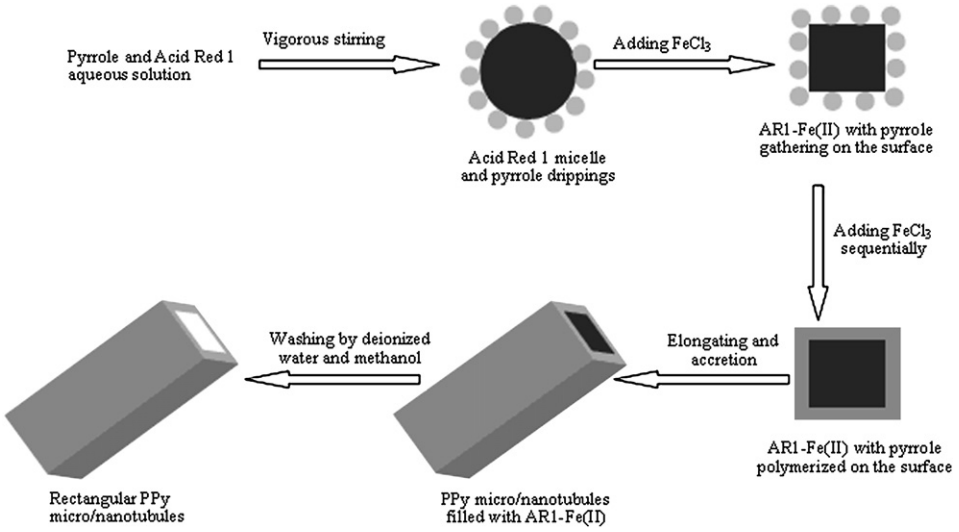

Fig. 11. Illustration of the formation mechanism of the rectangular-sectioned PPy micro/nanotubules via self-assembly using Acid Red 1 as dopant.

4. Conclusion

Aligned rectangular-sectioned PPy micro/nanotubules were synthesized via the self-assembly method using Acid Red 1 as dopant. It was found that the general morphology of PPy could be manipulated by varying the polymerization time, pyrrole monomer concentration, oxidant, and the stirring condition. Rectangular-sectioned and cylindrical PPy micro/nanotubules, and granular PPy were obtained at different conditions.

The synthesized rectangular-sectioned PPy tubules have an average length of 530 μm and a conductivity of 28.6 S/cm. Characterizations of PPy and reaction intermediates revealed the formation mechanism of different morphologies of PPy as: (1) when there was no stirring in the solution, AR1–Fe(II) crystals produced from the complexation of Fe^{2+} and Acid Red 1 precipitated as tetragonal crystals in the Acid Red 1 micelles, on which pyrrole monomers polymerized and rectangular-sectioned PPy micro/nanotubules formed via elongation and accretion; (2) when the solution is under vigorous stirring, the Acid Red 1 micelles acted as 'templates' and cylindrical PPy micro/nanotubules were obtained, which is similar to previous studies.

Acknowledgement

The authors gratefully acknowledge the financial support from National Natural Science Foundation of China (Grant No. 50276050).

References

[1] Akkerman HB, Blom PWM, de Leeuw DM, de Boer B. Nature 2006;441(7089):69–72.
[2] Sailor MJ, Curtis CL. Adv Mater 1994;6(9):688–92.
[3] Mortimer RJ, Dyer AL, Reynolds JR. Displays 2006;27(1):2–18.
[4] Roussel F, Chan-Yu-King R, Buisine JM. Eur Phys J E 2003;11(3):293–300.
[5] Ramanavicius A, Ramanaviciene A, Malinauskas A. Electrochim Acta 2006;51(27):6025–37.
[6] Gerard M, Chaubey A, Malhotra BD. Biosens Bioelectron 2002;17(5):345–59.
[7] Tess ME, Cox JA. J Pharmaceut Biomed 1999;19(1–2):55–68.
[8] Geetha S, Rao CRK, Vijayan M, Trivedi DC. Anal Chim Acta 2006;568(1–2):119–25.
[9] Liu J, Wan MX. J Polym Sci Part A Polym Chem 2001;39:997–1004.
[10] Nalwa HS, editor. Handbook of organic conductive molecules and polymers. Conductive polymers: synthesis and electrical properties, vol. 2. New York: John Wiley & Sons; 1997. p. 419–68.
[11] Chronakis IS, Grapenson S, Jakob A. Polymer 2006;47(5):1597–603.
[12] Yang XM, Dai TY, Lu Y. Polymer 2006;47(1):441–7.
[13] Martin CR. Science 1994;266(5193):1961–6.
[14] Koopal CGJ, Feiters MC, Nolte RJM, de Ruiter B, Schasfoort RBM. Biosens Bioelectron 1992;7(7):461–71.
[15] Demoustier-Champagne S, Duchet J, Legras R. Synth Met 1999;101:20–1.
[16] Liu L, Zhao CJ, Zhao YM, Jia NQ, Zhou Q, Yan MM, et al. Eur Polym J 2005;41(9):2117–21.
[17] Yang YS, Liu J, Wan MX. Nanotechnology 2002;13(6):771–3.
[18] Shen YQ, Wan MX. J Polym Sci Part A Polym Chem 1999;37(10):1443–9.
[19] Wei ZX, Zhang LJ, Yu M, Yang YS, Wan MX. Adv Mater 2003;15(16):1382–5.
[20] Yang YS, Wan MX. J Mater Chem 2001;11(8):2022–7.
[21] Dai TY, Yang XM, Lu Y. Nanotechnology 2006;17(12):3028–34.
[22] Jang J, Yoon H. Langmuir 2005;21(24):11484–9.
[23] Zhang LJ, Peng H, Hsu CF, Kilmartin PA, Travas-Sejdic J. Nanotechnology 2007;18(11):115607.
[24] Zhang XJ, Zhang XH, Shi WS, Meng XM, Lee C, Lee S. Angew Chem Int Ed 2007;46(9):1525–8.
[25] Han J, Yan W, Xu YB. Chem Lett 2006;35(3):306–7.
[26] Yun J, Choi H. Talanta 2000;52(5):893–902.
[27] Ai SF, He Q, Tao C, Zheng SP, Li JB. Macromol Rapid Commun 2005;26(24):1965–9.
[28] Acik M, Sonmez G. Polym Adv Technol 2006;17(9–10):697–9.
[29] Koo YK, Kim BH, Park DH, Joo J. Mol Cryst Liq Cryst 2004;425(1):55–60.
[30] Harada M, Adachi M. Adv Mater 2000;12(11):839–41.
[31] Kim BJ, Oh SG, Han MG, Im SS. Langmuir 2000;16(14):5841–5.
[32] (a) Yoon H, Chang M, Jang J. Adv Funct Mater 2007;17:431–6; (b) Yoon H, Chang M, Jang J. Adv Mater 2005;17:1616–20.
[33] Zoeller N, Blankschtein D. Langmuir 1998;14(25):7155–65.
[34] Nelson PH, Rutledge GC, Hatton TA. J Chem Phys 1997;107(24):10777–81.

[35] Gao HW. Talanta 2000;52(5):817–23.
[36] Visser AE, Griffin ST, Hartman DH, Rogers RD. J Chromatogr B 2000; 743(1–2):107–14.
[37] (a) Koprivanac N, Papic S, Grabaric Z, Osterman-Parac D, Mesinovic A. Dyes Pigments 1993;22(1):1–13;
(b) Yang XM, Zhu ZX, Dai TY, Lu Y. Macromol Rapid Commun 2005; 26(21):1736–40.
[38] Menon VP, Lei J, Martin CR. Chem Mater 1996;8(9):2382–90.
[39] Kros A, Nolte RJM, Sommerdijk NAJM. Adv Mater 2002;14(23): 1779–82.